Kinetics and products of HONO interaction with TiO2 surface under UV irradiation

ARTICLE *in* ATMOSPHERIC ENVIRONMENT · MARCH 2013

Impact Factor: 3.28 · DOI: 10.1016/j.atmosenv.2012.11.016

3 AUTHORS:

Atallah El Zein
Université du Littoral Côte d'Opale (ULCO)
13 PUBLICATIONS **119** CITATIONS
SEE PROFILE

Yuri Bedjanian
CNRS Orleans Campus
67 PUBLICATIONS **853** CITATIONS
SEE PROFILE

Manolis N Romanias
Ecole des Mines de Douai
25 PUBLICATIONS **99** CITATIONS
SEE PROFILE

Atmospheric Environment 67 (2013) 203–210

Contents lists available at SciVerse ScienceDirect

Atmospheric Environment

journal homepage: www.elsevier.com/locate/atmosenv

Kinetics and products of HONO interaction with TiO_2 surface under UV irradiation

Atallah El Zein, Yuri Bedjanian*, Manolis N. Romanias

Institut de Combustion, Aérothermique, Réactivité et Environnement (ICARE), CNRS, 45071 Orléans Cedex 2, France

HIGHLIGHTS

- Reactive uptake of HONO to UV irradiated TiO_2 surface was studied.
- Uptake coefficient was measured as function of temperature and relative humidity.
- NO_2 and NO were observed as reaction products with 52 and 48% yields, respectively.
- Daytime HONO loss on mineral aerosol is of minor importance in the atmosphere.

ARTICLE INFO

Article history:
Received 16 July 2012
Received in revised form
5 November 2012
Accepted 7 November 2012

Keywords:
TiO_2
HONO
Heterogeneous reaction
Uptake coefficient
Products

ABSTRACT

The interaction of HONO with UV irradiated TiO_2 solid films was studied using a low pressure flow reactor (1–10 Torr of Helium) combined with a modulated molecular beam mass spectrometer for monitoring of the gaseous species involved. The reactive uptake of HONO to TiO_2 was studied in absence of O_2 in the reactor as a function of HONO concentration ($[HONO]_0 = (0.5–5.0) \times 10^{12}$ molecule cm^{-3}), relative humidity (RH = 0.001–60%) and temperature (T = 275–320 K). The measured initial uptake coefficient (γ_0) of HONO on TiO_2 surface was independent of the HONO concentration and showed slight inverse dependence on temperature (activation factor = −1390 ± 150 K) and relative humidity: $\gamma_0 = 6.9 \times 10^{-4}$ $(RH)^{-0.3}$ (at T = 280 K, calculated using BET surface area, 30% uncertainty). NO_2 and NO were observed as products of the HONO reaction with UV irradiated TiO_2 surface with sum of their yields corresponding to nearly 100% of the nitrogen mass balance. The yields of the NO and NO_2 products were found to be (48 ± 7) and (52 ± 8) %, respectively, independent of relative humidity, temperature and concentration of HONO under experimental conditions used. The HONO loss on mineral aerosol during daytime (calculated with uptake data for HONO on TiO_2 surface in presence of UV irradiation) appears to be of minor importance compared with HONO photolysis in the atmosphere.

1. Introduction

Nitrous acid (HONO) is an important atmospheric species representing a significant daytime photochemical source of OH radical, the major atmospheric oxidant. Therefore, HONO affects the HO_x and NO_x budgets, which are the two key groups of species involved in ozone formation, and subsequently in the oxidative capacity of the troposphere (Calvert et al., 1994; Kerbrat et al., 2010; Lammel and Cape, 1996). Because of its rapid photolysis during daytime, elevated concentrations of HONO have been observed only at night, ranging from a few ppbv at polluted sites to 70 pptv in the Arctic (Appel et al., 1990; Li, 1994). In the clean troposphere during daytime, the steady state concentrations of HONO range from 100 to 500 pptv (Lammel and Cape, 1996; Vecera and Dasgupta, 1991). The mechanisms of HONO formation in the atmosphere are still not completely understood. One current issue in the chemistry of HONO is that models fail to reproduce unexpectedly high daytime concentrations of HONO observed in the field studies, suggesting the existence of new, yet unknown, daytime sources of HONO (Kleffmann, 2007). Heterogeneous processes, including those on humid surfaces, being thought to be the major source of HONO in the atmosphere, were intensively studied in the laboratory and several mechanisms of HONO formation on aerosol and ground surfaces have been proposed (Kleffmann, 2007).

In competition with heterogeneous HONO formation the atmospheric aerosol can also act as a sink for gaseous HONO. The kinetic and mechanistic data on HONO interaction with different surfaces seems to be very useful, not only for atmospheric implications but also for laboratory studies of the HONO forming heterogeneous processes where secondary surface reactions of HONO may have an impact on the occurring chemistry and final HONO yields. The available information on the nature, rate and

* Corresponding author. Tel.: +33 238255474; fax: +33 238696004.
E-mail address: yuri.bedjanian@cnrs-orleans.fr (Y. Bedjanian).

1352-2310/$ – see front matter © 2012 Elsevier Ltd. All rights reserved.
http://dx.doi.org/10.1016/j.atmosenv.2012.11.016

products of HONO interaction with solid surfaces of atmospheric interest is very scarce and seems to be limited to a few studies carried out with ice (Chu et al., 2000; Diao and Chu, 2005; Fenter and Rossi, 1996; Kerbrat et al., 2010) and soot surface (Lelièvre et al., 2004; Stadler and Rossi, 2000). Recently, we have reported the results of the experimental study of HONO interaction with TiO_2 under dark conditions (El Zein and Bedjanian, 2012b). In addition, there have been several studies of the loss of HONO on "laboratory" surfaces such as Pyrex (Kaiser and Wu, 1977; Ten Brink and Spoelstra, 1998), and borosilicate glass (Syomin and Finlayson-Pitts, 2003).

The present paper is one of a series on systematic study of the kinetics and products of the heterogeneous interaction of HONO with mineral aerosol and its different constituents, and is focused on the reaction of HONO with UV irradiated TiO_2 surface. Titanium dioxide, although being a minor component of mineral dust particles (Karagulian et al., 2006), was shown recently to be responsible for the photochemical reactivity of atmospheric mineral aerosols (Ndour et al., 2008). In addition, titanium dioxide is a very efficient photocatalyst which is known to transform nitrogen oxides (NO/NO_2), via catalytic heterogeneous reactions, to HNO_3 (Dalton et al., 2002; Devahasdin et al., 2003; Ibusuki and Takeuchi, 1994; Ohko et al., 2008). Due to these photocatalytic properties TiO_2 is widely used in a variety of so-called de-polluting building materials aimed at removing the nitrogen oxides from the atmosphere. Recently, the antipolluting nature of the TiO_2-containing materials was questioned (Langridge et al., 2009; Monge et al., 2010). In particular, it was shown that the interaction of NO_2 with TiO_2 (Bedjanian and El Zein, 2012; Monge et al., 2010) and commercial self-cleaning TiO_2-containig window glass (Langridge et al., 2009) results in the formation of nitrous acid in the gas phase. In contrast to mentioned studies, Laufs et al. (2010) working with TiO_2 doped commercial paints observed an efficient decomposition of HONO on the photolytic samples and concluded that the paint surfaces do not represent a source of HONO. On the basis of the above information, the experimental study of the interaction of HONO with TiO_2 under UV irradiation seems to be of great interest.

2. Experimental

Interaction of HONO with solid TiO_2 films was studied at 1–10 Torr total pressure (He being used as a carrier gas) in absence of O_2 in the reactive system using flow tube technique with mass spectrometric detection of the gaseous species involved. The experimental equipment and approach used for the kinetic measurements were described in previous papers from this group (Bedjanian and El Zein, 2012; El Zein and Bedjanian, 2012a; El Zein and Bedjanian, 2012b). The main reactor (Fig. 1) consisted of a Pyrex tube (40 cm length and 2.4 cm i.d.) with a jacket for the thermostated liquid circulation. The reactor was surrounded by 6 UV lamps (Sylvania BL350, 8 W, 315–400 nm with peak at 352 nm). The actinic flux inside the reactor was not measured in the present study, however, in order to characterize the irradiance intensity in the reactor we have directly measured the NO_2 photolysis frequency, J_{NO_2}, as a function of the number of lamps switched on. The values of J_{NO_2} were found to be between 0.002 and 0.012 s^{-1} for 1–6 lamps switched on, respectively (El Zein and Bedjanian, 2012a).

Solid TiO_2 films were deposited on the outer surface of a Pyrex tube (0.9 cm o.d.) using TiO_2 (Sigma Aldrich, Aeroxide P25, (50 ± 15) m^2 g^{-1} surface area, ~20 nm particle diameter) suspension in ethanol. Prior to film deposition, the Pyrex tube was treated with hydrofluoric acid and washed with distilled water and ethanol. Then the tube was immersed into the suspension, withdrawn and dried with a fan heater. As a result rather homogeneous (to eye) films of TiO_2 were formed at the Pyrex surface. In order to eliminate the possible residual traces of ethanol, prior to uptake experiments, the freshly prepared TiO_2 samples were heated at (100–150)°C during (20–30) min under pumping. Experiments were carried out using a coaxial configuration of the flow reactor with movable central injector: the Pyrex tube with deposited sample was introduced into the main reactor along its axis. The coated tube could be moved relative to the outer tube of the injector that allowed the variation of the solid film length exposed to gas phase reactant and consequently of the reaction time. In addition, the sample could be heated up to a few hundreds °C by means of a coaxial cylindrical heater which could be introduced inside the tube coated with the sample.

HONO was generated via heterogeneous reaction of HCl with $NaNO_2$:

$$HCl + NaNO_2 \rightarrow HONO + NaCl$$

HCl diluted in He flowed through a column containing $NaNO_2$ crystals, and heterogeneously formed HONO was injected through the reactor side arm and detected at its parent peak as $HONO^+$ ($m/z = 47$). Under the experimental conditions used this source of HONO was found to be free of residual concentration of HCl. Monitoring of the HCl concentration by mass spectrometry confirmed that HCl was completely consumed in reaction with $NaNO_2$ and did not reach the main reactor. This HONO source is known to be free of NO_2 and HNO_3 (Bedjanian et al., 2004). In the present work, no signals were detected at $m/z = 46$ (NO_2^+), 62 (NO_3^+), and 63 (HNO_3^+) when HONO was present in the reactor. However, measurable concentration of NO coming from the HONO source was detected (10–20% of [HONO]) in agreement with the results of a previous study (Bedjanian et al., 2004). Absolute concentrations of HONO were measured in situ using the method proposed previously (Bedjanian et al., 2004). This direct calibration method consisted of chemical conversion of HONO to NO_2 via the fast reaction with F atoms with subsequent detection and measurement of NO_2 concentration formed.

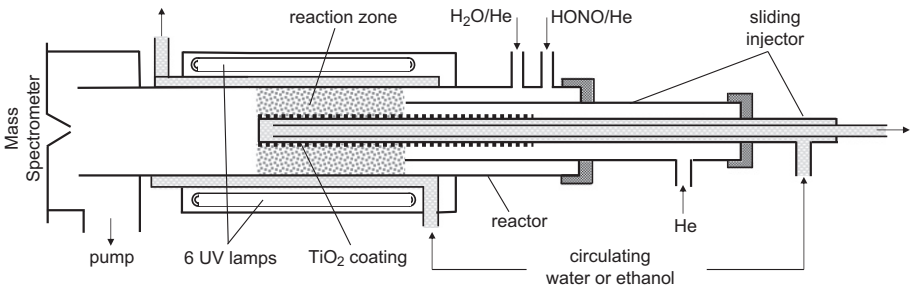

Fig. 1. Diagram of the flow photoreactor used.

H_2O was introduced into the reactor from a bubbler containing thermostated ($T = 298$ K) deionized water. The concentrations of H_2O in the reactor were determined by calculating the H_2O flow rate from the total (H_2O + He) and H_2O vapour pressures in H_2O bubbler and the measured flow rate of He through the bubbler. The lowest concentrations of water corresponding to RH down to 0.001% were determined using the absolute calibration of the mass spectrometer at $m/z = 18$ (H_2O^+). The estimated uncertainty on the determination of RH was nearly 15%, independent of its absolute value. The concentrations of the other stable species, in particular those of the reaction products NO and NO_2, were calculated from their flow rates obtained from the measurements of the pressure drop in calibrated volume flasks with the species diluted in helium. All species were detected at their parent peaks. NO^+ being a fragment of NO_2 and HONO, the NO signal at $m/z = 30$ was corrected for the fragmentation of NO_2 and HONO in the ion source of the mass spectrometer which operated at 25–30 eV. These corrections could be easily done by simultaneous detection of the signals from NO_2 at $m/z = 46$ and 30 and HONO at $m/z = 47$ and 30.

3. Results

3.1. Kinetics of HONO loss

Uptake coefficient of HONO (γ) defined as the probability of reactive HONO loss per collision with TiO_2 surface was calculated using the following expression:

$$\gamma = \frac{4k'}{\omega}\frac{V}{S}$$

where k' (s^{-1}) is the first-order rate constant of HONO loss, ω the average molecular speed, V the volume of the reaction zone, and S the surface area of the TiO_2 sample. To calculate the uptake coefficient, two parameters should be determined experimentally: the rate constant k' and TiO_2 film surface area accessible to HONO.

Fig. 2 (filled circles) displays an example of HONO consumption kinetics in heterogeneous reaction with TiO_2 surface. These data were obtained by varying the length of TiO_2 film in contact with HONO, which is equivalent to varying the reaction time. The decays of HONO were found to be exponential (solid line in Fig. 2) and were treated with the first-order kinetics formalism, the rate constant being determined as:

$$k'_{obs} = -\frac{d\ln([HONO])}{dt}$$

where t is the reaction time defined by the sample length/flow velocity ratio (the flow velocities were in the range 250–1350 cm s^{-1}). The values of the observed first-order rate constants, k'_{obs}, determined from the decays of HONO were corrected for the diffusion limitation in the HONO transport from the volume to the reactive surface of the reactor. The radial diffusion problem for the coaxial configuration of the reactor used in the present study was solved by Gershenzon and co-workers (Gershenzon et al., 1995, 1994):

$$\frac{1}{k'_{obs}} = \frac{1}{k'} + \frac{R^2}{K^d(q)D_0} \times P$$

where k' is a true rate constant, D_0 is the diffusion coefficient of HONO at 1 Torr pressure (Torr cm^2 s^{-1}), P is the total pressure in the reactor and $K^d(q)$ is a dimensionless rate constant of radial diffusion, which is a function of sample tube radius (r) to main reactor radius (R) ratio, $q = r/R = 0.375$ (for configuration used in the present study). The diffusion coefficient of HONO in He, $D_0 = (490 \pm 50)$ Torr cm^2 s^{-1} at $T = 300$ K, determined previously (El Zein and Bedjanian, 2012b), was used through this study assuming $T^{1.75}$-dependence of D_0 on temperature. Applied to k' diffusion corrections ranged from a few to nearly 50% (for the highest k').

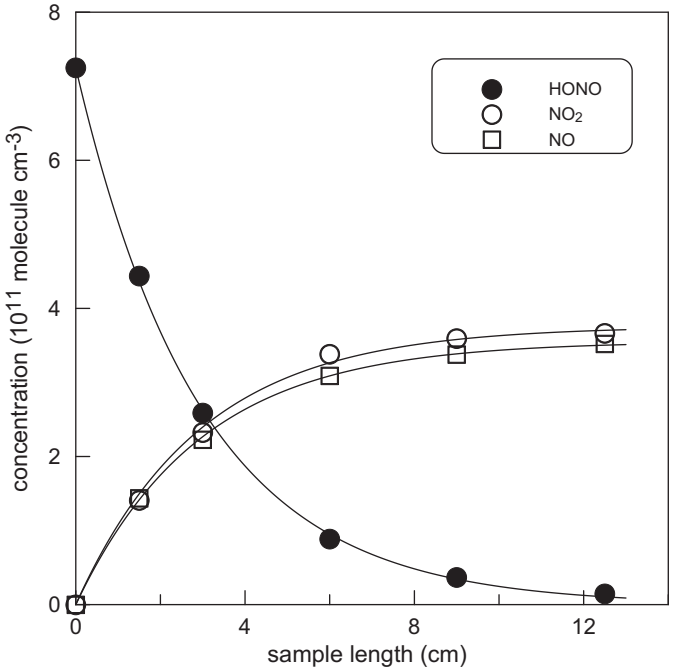

Fig. 2. Examples of kinetics of HONO consumption and products, NO and NO_2, formation in heterogeneous reaction of HONO with UV irradiated TiO_2 surface: $T = 300$ K, dry conditions, 6 lamps on ($J_{NO_2} = 0.012$ s^{-1}), mass of $TiO_2 = 0.1$ mg cm^{-1}.

The rate of HONO loss was found to decrease with exposure time indicating deactivation of TiO_2 sample during the heterogeneous reaction. For instance, the value of k' dropped by a factor of nearly 3 during 4 h exposure of 0.6 mg of TiO_2 to [HONO] = 1.0×10^{12} molecule cm^{-3} under dry conditions. Consequently, in the present study the measurements of the uptake coefficient were focused on its initial value corresponding to the first minute of the TiO_2 film exposure to HONO.

3.2. Dependence on sample mass

In these experiments, the HONO loss rate k' was measured as a function of the thickness of TiO_2 coating with the purpose to determine the TiO_2 surface area involved in the interaction with HONO under experimental conditions used. The results of the measurements of the initial rate of the HONO uptake to TiO_2 under dry conditions (RH = 0.001%) are shown in Fig. 3 as a dependence of the uptake coefficient of HONO (γ_{geom}, calculated with geometric, projected surface area) on the mass of TiO_2 deposited per unity length of the support tube (which is equivalent to the thickness of the coating). One can note that two regimes were observed: the first one, where γ_{geom} is linearly dependent on the mass of TiO_2 sample, and the second one (saturation region), where γ_{geom} is independent of the sample mass. We considered that linear dependence of the reaction probability on mass, hence thickness, of TiO_2 film indicates that the entire surface area of the solid sample is accessible to HONO and, consequently, the BET surface area should be used for calculations of the uptake coefficient. The uptake measurements in the present study were carried out with TiO_2

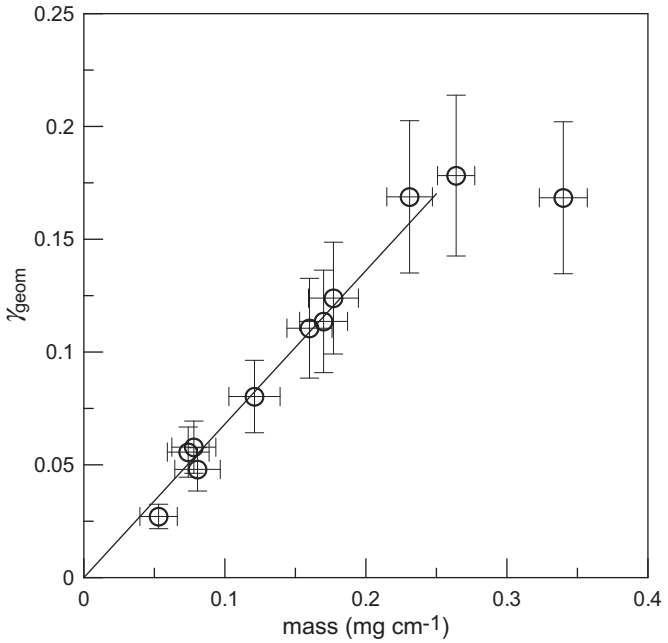

Fig. 3. Initial uptake coefficient of HONO (calculated using geometric surface area) as a function of the mass of TiO_2 sample (per 1 cm length of the support tube): $T = 300$ K, $P = 1$ Torr, dry conditions, $[HONO]_0 = (7–9) \times 10^{11}$ molecule cm^{-3}, $J_{NO_2} = 0.006$ s^{-1}.

sample masses below 0.25 mg cm^{-1}, where linear dependence of the reaction rate on sample mass was observed and BET surface area of the TiO_2 samples was used to determine γ. The linear dependence in Fig. 3 provides the following value of the initial uptake coefficient of HONO (for RH = 0.001%, $T = 300$ K, 6 lamps on):

$$\gamma_0 = (3.9 \pm 1.2) \times 10^{-3}$$

where uncertainty includes statistical one and those on BET surface area and on the measurements of k'. It should be noted that the value obtained for γ_0, being calculated with BET surface area, should be considered as a lower limit of the uptake coefficient.

3.3. Dependence on initial concentration of HONO and irradiation intensity

The initial rate of HONO loss was found to be independent of the HONO concentration. Thus in experiments carried out at $T = 300$ K, under dry conditions (RH = 0.001%) and with 6 lamps irradiation, for $[HONO]_0$ varied in the range $(4.9 \times 10^{11}–5.0 \times 10^{12})$ molecule cm^{-3} the measured values of the uptake coefficient were found to be similar within 15%: $\gamma_0 = (4.0 \pm 0.6) \times 10^{-3}$. The independence of the initial uptake coefficient of the HONO concentrations can be expected, considering that HONO loss rate depends on the number of active sites available on the surface and that these active sites are not yet occupied/destroyed at the initial stage of the surface exposure to HONO.

Similarly, it was observed that the uptake of HONO to TiO_2 surface is independent of the UV irradiation intensity. For instance, in a series of experiments carried out under dry conditions where interaction of HONO with TiO_2 surface was studied under irradiation with 1, 3 and 6 lamps (i.e. for J_{NO_2} between 0.002 and 0.012 s^{-1}) the measured values of γ_0 were in the range $(3.7 \pm 0.4) \times 10^{-3}$. This phenomenon of levelling of the uptake coefficient at high irradiation intensities was also observed in our previous study for the interaction of NO_2 with TiO_2 (El Zein and Bedjanian, 2012a).

3.4. Dependence on relative humidity

In this series of experiments the uptake coefficient of HONO was measured at $T = 280$ K as a function of relative humidity the former being varied by nearly 5 orders of magnitude: RH = 0.001–60%. Prior to uptake experiments (contact with HONO), the freshly prepared TiO_2 samples were heated under pumping (as noted in Experimental section) and then exposed during nearly 5 min to water vapour present in the reactor. The resulting inverse dependence of γ_0 on relative humidity is shown in Fig. 4. The solid line in Fig. 4 represents a power fit to the experimental data and corresponds to the following expression:

$$\gamma_0 = 6.9 \times 10^{-4}(RH)^{-0.3}$$

with estimated conservative 30% uncertainty on the uptake coefficient. The RH-dependence of the uptake coefficient of HONO to TiO_2 under dark conditions measured in our previous study (El Zein and Bedjanian, 2012b), $\gamma_0 = 1.8 \times 10^{-5}$ (RH)$^{-0.63}$, is also shown in Fig. 4 (dashed line) for comparison.

3.5. Temperature dependence

Temperature dependence of the uptake coefficient was measured in the temperature range (275–320) K under dry conditions, relative humidity being kept at a constant level (RH = 0.002%) at all the temperatures. The uptake coefficient was found to slightly decrease with increasing temperature (Fig. 5). The solid line in Fig. 5 represents an exponential fit to the experimental data and provides the following Arrhenius expression for γ_0:

$$\gamma_0 = \left(3.0 \pm 1.5\right) \times 10^{-5}\exp[(1390 \pm 150)/T]$$

at $T = 275–320$ K (uncertainties are 1σ statistical ones).

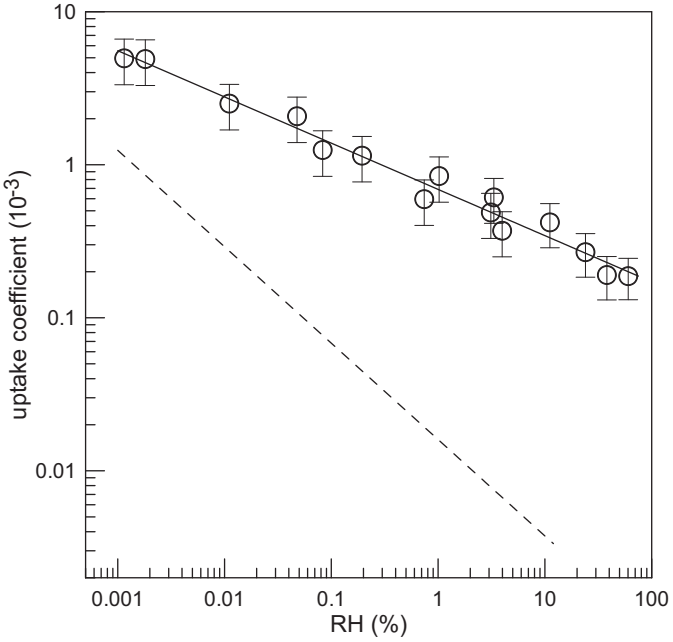

Fig. 4. Uptake coefficient as a function of relative humidity: $T = 280$ K, $P = 1–10$ Torr, $J_{NO_2} = 0.006$ s^{-1}. Dashed line represents the data observed under dark conditions (El Zein and Bedjanian, 2012b).

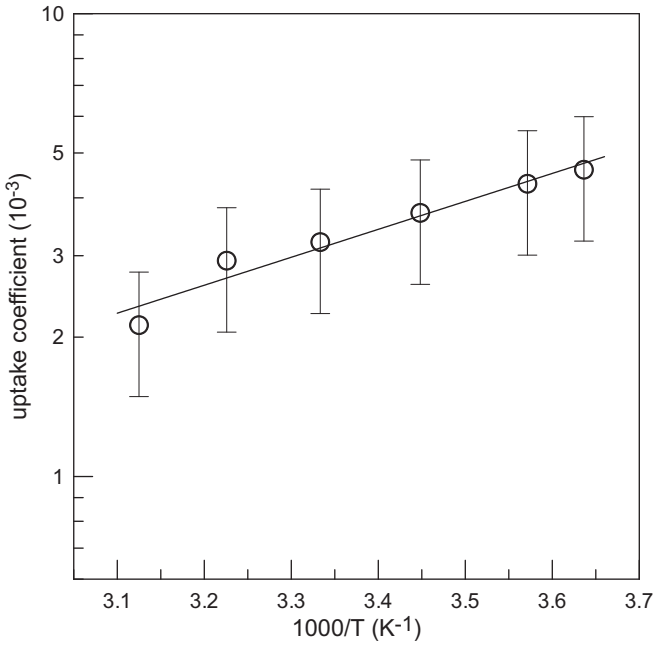

Fig. 5. Temperature dependence of the uptake coefficient measured under dry conditions (RH = 0.002%): $P = 1$ Torr, $T = 275$–320 K, $J_{NO_2} = 0.006$ s^{-1}.

3.6. Products study

NO and NO_2 were observed as gas phase products of the HONO interaction with UV irradiated TiO_2 surface. Fig. 2 shows the kinetics of products formation along with the kinetics of HONO decay. The solid lines depicting products kinetics represent fit to the experimental data according to the following equation

$$[\text{product}] = \alpha \times [\text{HONO}]_0 \times (1 - \exp(-k't))$$

where k' is the first order rate constant determined from the kinetics of HONO consumption and α is the branching ratio for the product forming reaction channel. The values of α obtained from the best fit to experimental data in Fig. 2 were 0.52 and 0.49 for NO_2 and NO, respectively, which corresponds to nearly 100% nitrogen mass balance.

Experiments described in this section were focused on the determination of the products of the interaction of HONO with TiO_2 surface under varied experimental conditions. Typical experiments consisted in the introduction of the TiO_2 sample into the reaction zone in contact with HONO and monitoring of the HONO concentration and those of the two gas phase products formed. The yield of the detected products was determined as a ratio of the product concentration formed to the concentration of HONO consumed: product yield = Δ[product]/Δ[HONO]. The yields of the reaction products were found to be dependent on the time of surface exposure to HONO. At the initial stage of the heterogeneous reaction high yield of NO (up to 70%) and relatively low yield of NO_2 (down to 20%) were sometimes observed depending on the experimental conditions (especially at high contact times resulting in almost total consumption of HONO). The yield of NO progressively decreased and that of NO_2 increased with exposure time approaching to their steady (nearly 50%) values which were no more changed with time. This observation is most likely due to an efficient NO forming reactive uptake of NO_2 to fresh TiO_2 sample at the initial stage of the reaction which decreases upon surface ageing (Bedjanian and El Zein, 2012; El Zein and Bedjanian, 2012a).

It should be noted that all the measurements presented below were conducted under "stabilised" steady state product yield conditions.

Fig. 6 shows the concentrations of NO and NO_2 formed in the reaction of HONO with TiO_2 surface as a function of the consumed concentration of HONO. Initial concentration of HONO in these experiments was varied in the range $(0.7–6.0) \times 10^{12}$ molecule cm^{-3}. The data presented in Fig. 6 were measured at different temperatures in the reactor: 275, 300 and 320 K (three measurements at each temperature). The impact of temperature on the distribution of the reaction products was found to be negligible under the experimental conditions used. The straight lines in Fig. 6 correspond to the linear through origin least-squares fits to the experimental data and provide the branching ratios of 52.2 and 48.1% for NO_2 and NO forming pathways, respectively.

Fig. 7 displays the dependence of the products yield on the concentration of H_2O present in the reactor. The variation of the concentration of water by three orders of magnitude was found to have no impact on the yield of products of the heterogeneous reaction. The dashed lines in Fig. 7 correspond to mean values of the NO_2 and NO yields measured in these experiments: 52.5 and 48.3%, respectively.

In order to verify if some species are not released into the gas phase during the heterogeneous reaction and remain on the surface, we have carried out a few qualitative experiments consisting in heating (up to 250 °C) or UV irradiation of the HONO reacted TiO_2 samples with simultaneous monitoring of the species emitted into the gas phase. In these experiments, the solid film of TiO_2 was first treated with HONO under UV irradiation during a certain time, then pumped in a flow of helium and finally heated or irradiated. HONO/NO_2 and NO_2/NO were observed in the gas phase upon heating and UV irradiation of the reacted sample, respectively. Concerning surface concentration of non reacted HONO, thermal desorption experiments of the post reacted samples (being exposed to HONO from 1 to 30 min) showed that

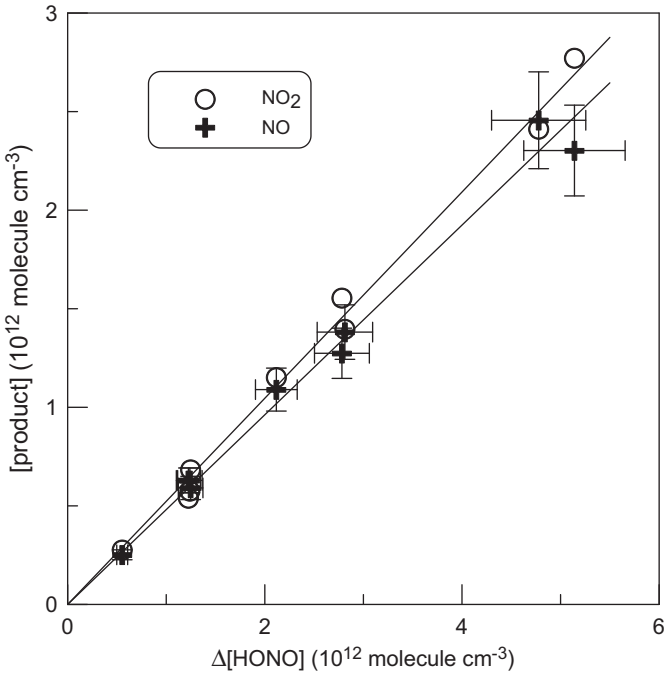

Fig. 6. Dependence of the concentration of the products formed on the concentration of HONO consumed measured with initial concentration of HONO varied in the range $(0.7–6.0) \times 10^{12}$ molecule cm^{-3} and at three different temperatures in the reactor: 275, 300 and 320 K. Error bars represent estimated uncertainties on the measurements of the absolute concentrations of the species.

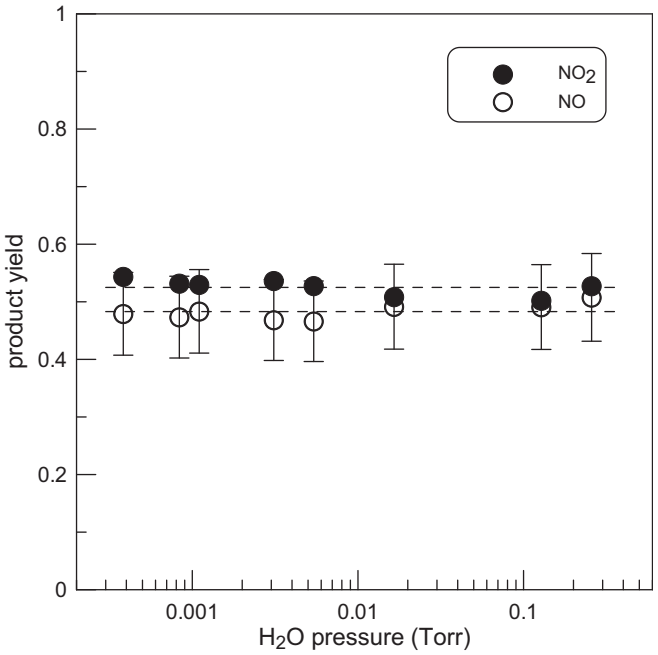

Fig. 7. Branching ratio of the NO_2 and NO forming pathways (estimated 15% uncertainties are shown for the case of NO) of the reaction of HONO with TiO_2 surface measured at different concentrations of water: $T = 280$ K, $J_{NO_2} = 0.012$ s^{-1}.

surface HONO levelled off (even at lowest exposure time of 1 min) at a steady-state value of nearly 2.8×10^{12} molecule cm^{-2} (calculated using BET surface area). NO and NO_2 were found to be released into the gas phase upon irradiation of the reacted surface: their concentrations increased rapidly upon turning UV lamps on ($t = 0$ in Fig. 8) and then decreased with time of irradiation. Fig. 8 shows an example of such temporal profiles for NO. Exponential fit of the observed profiles of NO (solid lines in Fig. 8) provides the values of 1.4 and 2.8 min^{-1} for the rates of decrease of NO concentration with time upon surface irradiation with 1 and 2 lamps, respectively. Assuming that desorption of NO is much more rapid process compared with its production reaction on the surface, this rate of decrease of NO concentrations in the gas phase can be attributed to the photolytic consumption of the surface adsorbed reactants (most likely HONO and/or NO_2) leading to the formation of NO.

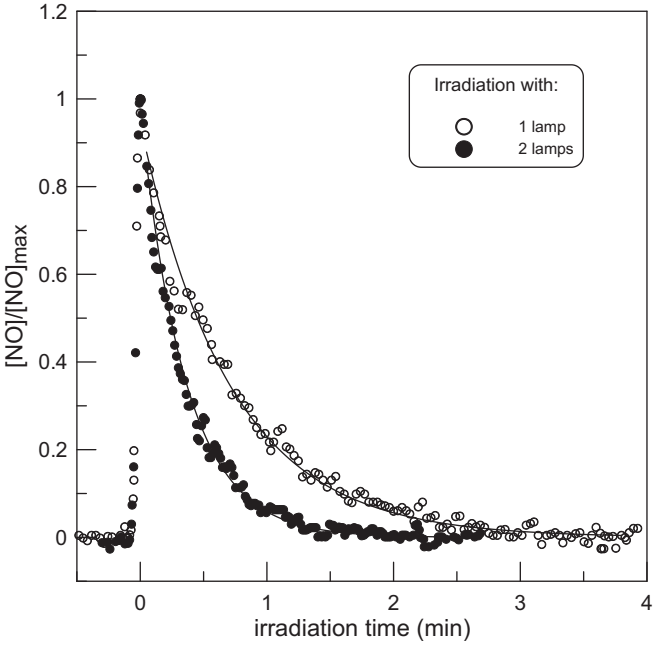

Fig. 8. Normalized concentration of NO observed in the gas phase upon irradiation of TiO_2 sample treated with HONO during 10 min.

4. Discussion

4.1. Comparison with previous data

In the present study, two gas phase products, NO_2 and NO, were found to be formed in the heterogeneous reaction of HONO with TiO_2 surface with equal, in the range of experimental uncertainty, nearly 50% yields. The branching ratios for the NO and NO_2 forming reaction pathways were shown to be independent of temperature and water pressure. Close results were reported by Syomin and Finlayson-Pitts (2003) who observed equal yields for NO and NO_2 in their unconditioned borosilicate glass cell under dry dark conditions. The formation of the equal amounts of NO and NO_2 was suggested to proceed via autoionization reaction between gas-phase and adsorbed HONO:

$$HONO_g + HONO_{ads} \rightarrow NO^+ + NO_2^- + H_2O \quad (1)$$

$$NO^+ + NO_2^- \rightarrow N_2O_3 \rightarrow NO + NO_2 \quad (2)$$

The product data from the present study is in agreement with the prediction of this mechanism. However, additional (to those on glass surface) reaction pathways can be expected to occur on more complex and more reactive TiO_2 surface under UV irradiation. The absorbed UV light activates the surface of photocatalyst promoting an electron to the conduction band and leaving a hole in the valence band:

$$TiO_2 + h\nu \rightarrow h^+ + e^- \quad (3)$$

The electrons and holes formed can lead to the reduction and oxidation reactions of HONO, for example, via reactions (4) and (5), forming NO_2 and NO, the observed reaction products:

$$HONO + h^+ \rightarrow NO_2 + H^+ \quad (4)$$

$$HONO + H^+ + e^- \rightarrow NO + H_2O \quad (5)$$

The rate of HONO heterogeneous loss was found to be independent of the UV irradiation intensity. This observation seems to point out that the rate limiting step of the reaction is the adsorption rate of HONO on the surface, which is actually measured in the work as reactive uptake of HONO.

Negative dependence both on temperature and relative humidity was found for the initial uptake coefficient of HONO to TiO_2 surface in the present study. Similar effect of the decrease of the HONO loss rate with increasing RH was observed in previous studies carried out with glass surfaces (Kaiser and Wu, 1977; Syomin and Finlayson-Pitts, 2003). The negative dependence of the HONO uptake rate on concentration of water was attributed to competition between HONO and H_2O for the available surface sites (Syomin and Finlayson-Pitts, 2003). Comparison of the data presented in Fig. 4 for RH dependence of HONO uptake to TiO_2 under irradiation and dark conditions shows that significantly stronger RH dependence was observed for uptake coefficient under dark conditions. Probably, under UV irradiation the effect of blocking the surface active sites by water is partly compensated by the role of water as a source of active species on the irradiated surface:

$$h^+ + H_2O \rightarrow OH + H^+ \quad (6)$$

The products of reaction (6), H^+ and OH radicals, react with HONO through reactions (5) and (7), forming NO and NO_2, respectively:

$$OH + HONO \rightarrow NO_2 + H_2O \quad (7)$$

This reaction sequence is in line with the experimental observation of the independence of the product yields of the relative humidity. It is clear that complete reaction mechanism is much more complex than the proposed set of reactions, even though it fits the experimental findings. To have more insight into the reaction mechanism additional information is needed, especially on the evolution of the chemical composition of the surface during the heterogeneous reaction.

To our knowledge, this is the first direct study of the heterogeneous interaction of HONO with UV irradiated mineral oxide surface. Laufs et al. (2010) studying NO_2 interaction with TiO_2 doped commercial paints observed nitrous acid formation in the dark and its efficient decomposition under UV irradiation. For the photolytic uptake coefficient of HONO the value of $\gamma = (2–9) \times 10^{-5}$ was determined (for RH in the range 10–85%). These values are lower than those measured in the present study: $\gamma \approx 3.4 \times 10^{-4}$ and $\approx 1.8 \times 10^{-4}$ at RH = 10 and 85%, respectively. In addition, in contrast to the present data the uptake of HONO was found to increase with increasing humidity. The decomposition of HONO on the photolytic samples was attributed to hydrolysis of HONO following by further oxidation of NO_2^- formed (Laufs et al., 2010):

$$HONO + H_2O \leftrightarrow NO_2^- + H_3O^+$$

It seems that this mechanism is not operative for pure TiO_2 samples used in the present study, where significant decrease of the HONO uptake rate with increasing RH was observed.

4.2. Atmospheric implications

The results obtained for the uptake of HONO on TiO_2 surface can be discussed in relation to atmospheric HONO chemistry occurring on aerosols and different types of ground surfaces. Concerning dark reaction, in our recent study (El Zein and Bedjanian, 2012b) the potential loss of HONO on aerosol surface was estimated using the experimental data for TiO_2 and compared with HONO loss due to dry deposition which is the main HONO sink process during nighttime. It was shown that the calculated rate of HONO loss on aerosols is much lower (at least by a factor of 50) than the dry deposition rate of HONO. The experimental data obtained in the present study for HONO uptake on UV irradiated surface of TiO_2 can be applied to assess the potential role of HONO loss on mineral aerosols during daytime. Using the value of $\gamma = 2.3 \times 10^{-4}$ measured at 40% RH with 1–6 UV lamps switched on (J_{NO_2} = 0.002–0.012 s^{-1}), aerosol surface loading of 10^{-6}–10^{-5} cm^{-1} (Seinfeld and Pandis, 1998; Wehner and Wiedensohler, 2003), typical for rural and urban atmosphere and in accordance with the expression:

$$k' = \frac{\omega\gamma}{4}\frac{S}{V}$$

the calculated value of HONO loss rate on aerosols is: $k' \sim (2 \times 10^{-6} - 2 \times 10^{-5})$ s^{-1} (for RH = 40%, T = 300 K). As one could expect, these numbers are too low compared to the photolysis rate of HONO which is $\sim(0.4–2.3) \times 10^{-3}$ s^{-1} under similar irradiation conditions (Kraus and Hofzumahaus, 1998). In addition, it should be mentioned that the rate of heterogeneous loss of HONO was calculated with the uptake data for TiO_2, which is the most reactive constituent of mineral aerosol. Thus the contribution of aerosol to the total HONO loss in the atmosphere both during daytime and nighttime can be considered as negligible. It should be noted that this conclusion is based on the data obtained in the absence of oxygen in the reactive system. In fact, the experimental system used in this study is not suitable for use under high concentrations of O_2. However, the presence of oxygen is not expected to significantly accelerate the heterogeneous reaction. It may even reduce the rate of this reaction as O_2 is known to be an efficient scavenger of electrons on the photocatalyst surface.

In relation to the de-polluting nature of the TiO_2 doped materials, present results on the reaction products show that even if HONO is taken up by these materials it is stoichiometrically converted to NO_x. However, it seems that to fully clarify the question, direct measurements of the rate and products of HONO interaction with individual TiO_2 containing de-polluting materials should be carried out on case by case basis.

Acknowledgements

This study was supported by LEFE – CHAT programme of CNRS (Photona project) and ANR from Photodust grant.

References

Appel, B.R., Winer, A.M., Tokiwa, Y., Biermann, H.W., 1990. Comparison of atmospheric nitrous acid measurements by annular denuder and differential optical absorption systems. Atmospheric Environment Part A General Topics 24, 611–616.

Bedjanian, Y., El Zein, A., 2012. Interaction of NO_2 with TiO_2 surface under UV irradiation: products study. Journal of Physical Chemistry A 116, 1758–1764.

Bedjanian, Y., Lelièvre, S., Bras, G.L., 2004. Kinetic and mechanistic study of the F atom reaction with nitrous acid. Journal of Photochemistry and Photobiology A: Chemistry 168, 103–108.

Calvert, J., Yarwood, G., Dunker, A., 1994. An evaluation of the mechanism of nitrous acid formation in the urban atmosphere. Research on Chemical Intermediates 20, 463–502.

Chu, L., Diao, G., Chu, L.T., 2000. Heterogeneous interaction and reaction of HONO on ice films between 173 and 230 K. Journal of Physical Chemistry A 104, 3150–3158.

Dalton, J.S., Janes, P.A., Jones, N.G., Nicholson, J.A., Hallam, K.R., Allen, G.C., 2002. Photocatalytic oxidation of NO_x gases using TiO_2: a surface spectroscopic approach. Environmental Pollution 120, 415–422.

Devahasdin, S., Fan Jr., C., Li, K., Chen, D.H., 2003. TiO_2 photocatalytic oxidation of nitric oxide: transient behavior and reaction kinetics. Journal of Photochemistry and Photobiology A: Chemistry 156, 161–170.

Diao, G., Chu, L.T., 2005. Heterogeneous reactions of HX + HONO and I_2 on ice surfaces: kinetics and linear correlations. Journal of Physical Chemistry A 109, 1364–1373.

El Zein, A., Bedjanian, Y., 2012a. Interaction of NO_2 with TiO_2 surface under UV irradiation: measurements of the uptake coefficient. Atmospheric Chemistry and Physics 12, 1013–1020.

El Zein, A., Bedjanian, Y., 2012b. Reactive uptake of HONO to TiO_2 surface: "dark" reaction. Journal of Physical Chemistry A 116, 3665–3672.

Fenter, F.F., Rossi, M.J., 1996. Heterogeneous kinetics of HONO on H_2SO_4 solutions and on ice: activation of HCl. Journal of Physical Chemistry 100, 13765–13775.

Gershenzon, Y.M., Grigorieva, V.M., Zasypkin, A.Y., Remorov, R.G., 1994. Theory of Radial Diffusion and First Order Wall Reaction in Movable and Immovable Media, Proceedings of the 13th International Symposium on Gas Kinetics. Book of Abstracts. University of Dublin, Dublin, Ireland, pp. 420–422.

Gershenzon, Y.M., Grigorieva, V.M., Ivanov, A.V., Remorov, R.G., 1995. O_3 and OH sensitivity to heterogeneous sinks of HO_x and CH_3O_2 on aerosol particles. Faraday Discussions 100, 83–100.

Ibusuki, T., Takeuchi, K., 1994. Removal of low concentration nitrogen oxides through photoassisted heterogeneous catalysis. Journal of Molecular Catalysis 88, 93–102.

Kaiser, E.W., Wu, C.H., 1977. A kinetic study of the gas phase formation and decomposition reactions of nitrous acid. Journal of Physical Chemistry 81, 1701–1706.

Karagulian, F., Santschi, C., Rossi, M.J., 2006. The heterogeneous chemical kinetics of N_2O_5 on $CaCO_3$ and other atmospheric mineral dust surrogates. Atmospheric Chemistry and Physics 6, 1373–1388.

Kerbrat, M., Huthwelker, T., Gäggeler, H.W., Ammann, M., 2010. Interaction of nitrous acid with polycrystalline ice: adsorption on the surface and diffusion into the bulk. Journal of Physical Chemistry C 114, 2208–2219.

Kleffmann, J., 2007. Daytime sources of nitrous acid (HONO) in the atmospheric boundary layer. Chem Phys Chem 8, 1137–1144.
Kraus, A., Hofzumahaus, A., 1998. Field measurements of atmospheric photolysis frequencies for O_3, NO_2, HCHO, CH_3CHO, H_2O_2, and HONO by UV spectroradiometry. Journal of Atmospheric Chemistry 31, 161–180.
Lammel, G., Cape, J.N., 1996. Nitrous acid and nitrite in the atmosphere. Chemical Society Reviews 25, 361–369.
Langridge, J.M., Gustafsson, R.J., Griffiths, P.T., Cox, R.A., Lambert, R.M., Jones, R.L., 2009. Solar driven nitrous acid formation on building material surfaces containing titanium dioxide: a concern for air quality in urban areas? Atmospheric Environment 43, 5128–5131.
Laufs, S., Burgeth, G., Duttlinger, W., Kurtenbach, R., Maban, M., Thomas, C., Wiesen, P., Kleffmann, J., 2010. Conversion of nitrogen oxides on commercial photocatalytic dispersion paints. Atmospheric Environment 44, 2341–2349.
Lelièvre, S., Bedjanian, Y., Laverdet, G., Le Bras, G., 2004. Heterogeneous reaction of NO_2 with hydrocarbon flame soot. Journal of Physical Chemistry A 108, 10807–10817.
Li, S.-M., 1994. Equilibrium of particle nitrite with gas phase HONO: tropospheric measurements in the high Arctic during polar sunrise. Journal of Geophysical Research 99, 25469–25478.
Monge, M.E., D'Anna, B., George, C., 2010. Nitrogen dioxide removal and nitrous acid formation on titanium oxide surfaces-an air quality remediation process? Physical Chemistry Chemical Physics 12, 8991–8998.
Ndour, M., D'Anna, B., George, C., Ka, O., Balkanski, Y., Kleffmann, J., Stemmler, K., Ammann, M., 2008. Photoenhanced uptake of NO_2 on mineral dust: laboratory experiments and model simulations. Geophysical Research Letters 35, L05812.
Ohko, Y., Nakamura, Y., Fukuda, A., Matsuzawa, S., Takeuchi, K., 2008. Photocatalytic Oxidation of Nitrogen Dioxide with TiO_2 Thin films under continuous UV-light illumination. Journal of Physical Chemistry C 112, 10502–10508.
Seinfeld, J.H., Pandis, S.N., 1998. Atmospheric Chemistry and Physics. Wiley-Interscience, New York.
Stadler, D., Rossi, M.J., 2000. The reactivity of NO_2 and HONO on flame soot at ambient temperature: the influence of combustion conditions. Physical Chemistry Chemical Physics 2, 5420–5429.
Syomin, D.A., Finlayson-Pitts, B.J., 2003. HONO decomposition on borosilicate glass surfaces: implications for environmental chamber studies and field experiments. Physical Chemistry Chemical Physics 5, 5236–5242.
Ten Brink, H.M., Spoelstra, H., 1998. The dark decay of hono in environmental (SMOG) chambers. Atmospheric Environment 32, 247–251.
Vecera, Z., Dasgupta, P.K., 1991. Measurement of ambient nitrous acid and a reliable calibration source for gaseous nitrous acid. Environmental Science & Technology 25, 255–260.
Wehner, B., Wiedensohler, A., 2003. Long term measurements of submicrometer urban aerosols: statistical analysis for correlations with meteorological conditions and trace gases. Atmospheric Chemistry and Physics 3, 867–879.